

## Spectral Element Approach for Inverse Models of 3D Layered Pavement

Chun-Ying. Wu<sup>1</sup>, R. Al-Khoury<sup>2</sup>, C. Kasbergen<sup>2</sup>, Xue-Yan. Liu<sup>2</sup>, and A. Scarpas<sup>2</sup>

**Abstract:** 3D spectral element method in the article is presented to predict the pavement layer modules using field measurement of Falling Weight Deflectometer (FWD). To improve the computational efficiency of the layer-condition assessment, one type of spectral element is proposed to develop the dynamic analysis of 3D multi-layered system subjected to an impulsive load. Each layer in structure is simulated as two-noded layer spectral element or one-noded spectral element in frequency domain. In order to identify the parameters of layered structures, a nonlinear optimization method called Powell hybrid algorithm is employed. The optimization procedure is performed in frequency domain and aims at minimizing the discrepancy of measured and calculated transfer function. In the case of the inverse calculation, it was verified that the Powell's algorithm had obtained stable and efficient convergences at the angle frequencies ranging from 10 Hz to 80 Hz. The new dynamic method was applied in the Continuously Reinforced Concrete Pavement(CRCP) project which has four layers. Compared with static method, it proved that the inversed-analytical results of the 3D spectral element dynamic method is more accurate and stable.

**Keyword:** 3D spectral element, Falling Weight Deflectometer (FWD), Continuously Reinforced Concrete Pavement (CRCP)

### 1 Introduction

Non-destructive dynamic testing is nowadays a well-recognized method for evaluating the struc-

tural capacity of pavements. Falling Weight Deflectometer (FWD) is one type of commonly used nondestructive tests. Most of computer programs used today for the parameter identification are based on the static analysis. In static analysis, only the maximal values of measured deflections are employed, which often leads to the incorrect results of the strength of rigid pavement layers and subgrade. However, when applying dynamic analysis, the computational efficiency always becomes a big concern in the inverse calculation. Dynamic Finite Element Method, usually an effective numerical method, can analyze complicated models with different geometries and loading conditions. However, due to its discrete characteristics of element meshes, FEM is difficult to be utilized in backcalculations. On the other hand, the analytical dynamic method, though very efficient, is usually cumbersome to treat complicated geometries and boundary conditions. Therefore, semi-analytical method is proposed for the forward and inverse dynamic model of 3D layered pavement structure.

Spectral element method developed by Doyle is one class of semi-analytical method. The algorithm describes waveguides in the element as the superposition of incident waves and reflection waves. Following this theory, Doyle (1997) applied spectral analysis mainly for the 1-D waveguides, Rizzi (1992) focused the work on the response of the wave propagation in 2-D layered solids, and Al-Khoury (2001) utilized the spectral element to analyze the dynamic impact of FWD load pulses on pavements. However, previous work only solved dynamic problems in the 2-D or semi-infinite multi-layered system.

A new type of spectral element was developed for three-dimensional layer system. Two types of spectral elements, two-noded layer spectral

<sup>1</sup> Jiangsu Transportation Institute, Nanjing, Jiangsu, wu\_chunying@hotmail.com

<sup>2</sup> Section of Structural Mechanics, Faculty of Civil Engineering and Geosciences, Delft University of Technology, Delft, Netherlands

element and one-noded throw-off spectral element were presented by Wu (2006) to calculate the models of three-layered pavement. In this study, Powell hybrid nonlinear optimization is introduced for the inverse algorithm and the objective function is constructed through the discrepancy between theoretical and measured transfer function. Backcalculation of identifying layer parameters is achieved by the minimized determination of the objective function. The inverse system of the new dynamic method is applied in CRCP pavement FWD measurement for the quality evaluation of pavement layers.

### 2 3D layer spectral element

3D layer spectral element is proposed for the three-dimensional layered structure subjected to FWD pulse load (Fig. 1). In the spectral analysis, one layer of the structure is treated as one layer spectral element. Two types of 3D spectral elements are developed for the layer structure, two-noded layer spectral element (Fig. 2) and one-noded throw-off spectral element (Fig. 3). In two-noded elements, two nodes are put to the center of upper surface and bottom surface; in one-noded element, one node is set to the center of upper surface. Generally, the last layer can be treated as a one-noded throw-off element if its thickness is large enough.

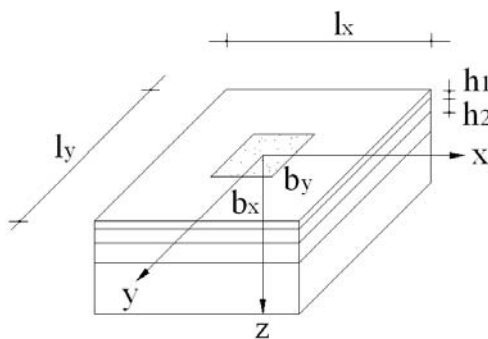


Figure 1: Structure of 3D layer pavement system

When homogeneous isotropic elastic solid with constant elastic material properties subjected to dynamic loads, there are two types of body waves: dilatational (P) wave and shear (S) wave. By the

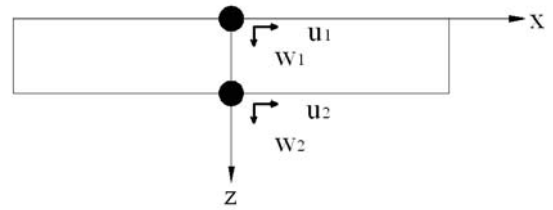


Figure 2: Two-noded layer element

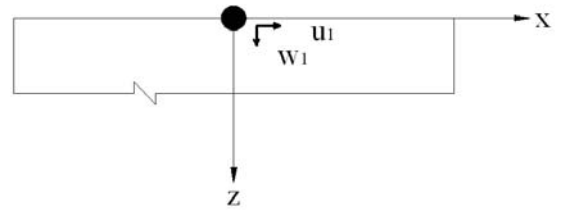


Figure 3: One-noded throw-off element

method of the separation of variables, the potentials are separated into three independent parts including components  $x$ ,  $y$  and  $z$ . The potentials become

$$\begin{aligned} \tilde{\varphi} &= \tilde{\varphi}(z) \cdot e^{-ik_r x} \cdot e^{-ik_m y} \\ \tilde{\psi} &= \tilde{\psi}(z) \cdot e^{-ik_r x} \cdot e^{-ik_m y} \end{aligned} \quad (1)$$

$k_r$  and  $k_m$  are independent variables defined as the roots of  $x$  and  $y$  direction in plate respectively.  $k_{zp}$  and  $k_{zs}$  are defined as wavenumbers of the P and S waves. The following relationships hold:

$$\begin{aligned} k_{zp} &= \left( \frac{\omega_n^2}{C_p^2} - k_r^2 - k_m^2 \right)^{1/2} \\ k_{zs} &= \left( \frac{\omega_n^2}{C_s^2} - k_r^2 - k_m^2 \right)^{1/2} \end{aligned} \quad (2)$$

Here  $\omega_n$  is angle frequency.  $C_p$  and  $C_s$  are the wave velocities of P and S waves.

#### 2.1 Two-noded layer spectral element

In two-nodal layer spectral element, each node has three degrees of freedom in  $x$ ,  $y$  and  $z$  directions, respectively. Due to the limited depth of  $z$  direction in a layer element, the vertical response

of wave at any node can be considered as the superposition of the incident wave and the reflection wave. Applying the superposition method, the potentials  $\tilde{\varphi}(z)$  and  $\tilde{\psi}(z)$  in the two-noded layer element is the summation of the potentials in the positive  $z$  direction and those in the negative  $z$  direction, which is expressed as follows:

$$\begin{aligned}\tilde{\varphi}(z) &= A \cdot e^{-ik_z p z} + B \cdot e^{-ik_z p (h-z)} \\ \tilde{\psi}(z) &= C \cdot e^{-ik_{zs} z} + D \cdot e^{-ik_{zs} (h-z)}\end{aligned}\quad (3)$$

In these two equations, the first terms in the brackets represent the incident wave propagating from the upper surface at  $z = 0$  and the second terms represent the reflected wave propagating from the boundary at  $z = h$ , where  $h$  is the thickness of the layer element.

When Substituting the potential equations into the displacement equations and taking the conditions of  $z = 0$  at node 1 and  $z = h$  at node 2 into the equations, the relations between the nodal displacement vector  $\tilde{u}$  and the coefficient vector  $\tilde{a}$  are expressed in the matrix style as follows:

$$\tilde{u} = \tilde{N} \cdot \tilde{a} \quad (4)$$

Inversing the Eq. 4, it becomes:

$$\tilde{a} = \frac{\tilde{M}}{\Delta} \cdot \tilde{u} \quad (5)$$

where the square matrix is defined as  $\tilde{N}^{-1} = \tilde{M}/\Delta$ .  $\Delta$  is the determinant of the matrix  $\tilde{N}$ . Substituting the potential equations into the stress equations, the stress matrix becomes:

$$\tilde{T} = \mu \cdot \tilde{P} \cdot \tilde{a} = \mu \cdot \frac{\tilde{P} \cdot \tilde{M}}{\Delta} \cdot \tilde{u} = (\mu/\Delta) \cdot \tilde{k} \cdot \tilde{u} \quad (6)$$

here  $\tilde{k} = \tilde{P} \cdot \tilde{M}$

$\tilde{k}$ , the matrix relating nodal force to nodal displacement, is analogous to the dynamic element stiffness in the conventional finite element method.

## 2.2 One-noded throw-off spectral element

The one-noded throw-off spectral element (Fig. 3) is a semi-infinite element. It is assumed that the wave only propagates in the negative  $z$  direction. Due to the absence of reflected wave in the

throw-off element, the potentials of dilatational and shear waves can be simplified by equalizing the coefficients  $B$  and  $D$  zero.

$$\begin{aligned}\tilde{\varphi}(z) &= A \cdot e^{-ik_z p z} \\ \tilde{\psi}(z) &= C \cdot e^{-ik_{zs} z}\end{aligned}\quad (7)$$

In the similar way as the two-noded layer element, a dynamic stiffness matrix can be formulated for the one-noded spectral element.

The behavior associated with Rayleigh waves is only observed after the coefficients have been determined by such equations as Eq.(5) (Rizzi, 1992). It is obvious that the single mode in the spectral response does in fact superposed to give the Rayleigh surface wave. The other components are necessary for the complete solution of the location near the impact site.

## 3 Assemblage of the global stiffness matrix and spectral structure

Under the condition that the displacements are compatible between two elements, the global stiffness matrix is assembled by some layer elements and one throw-off element. The rule of assemblage is similar to the conventional finite element method. The global equation is expressed as:

$$[\tilde{K}(z, k_r, k_m, \omega_n)] \cdot \tilde{U} = \tilde{P} \quad (8)$$

$[\tilde{K}(z, k_r, k_m, \omega_n)]$  is the global stiffness matrix.  $\tilde{U}$  is the global displacement vector, and  $\tilde{P}$  is the global force vector. These two vectors in frequency domain can be evaluated by the displacement and stress boundary conditions. If  $\tilde{P}$  only includes the vertical displacement at the first node in the whole layer structure,  $\tilde{P}$  will become a unit vector. Then the in-time displacement becomes:

$$u_i(x, y, t) = \sum_n \sum_m \sum_r A \cdot \tilde{G} \cdot \tilde{F}_{rm} \cdot \cos(k_r x) \cdot \cos(k_m y) \cdot \tilde{F}_n \cdot e^{i\omega_n t} \quad (9)$$

in which  $\tilde{G}$  is the inverse matrix of  $\tilde{K}$ ,  $A$  is the area of the applied load,  $\tilde{F}_{rm}$  is the coefficient of the spatial distribution of the applied load, and  $\tilde{F}_n$  is the time variation coefficient that is determined by the theory of Fast Fourier Transforms (FFT).

#### 4 Determination of $\tilde{F}_{rm}$

A pulse load can be separated into two independent functions, then

$$P[(x,y),t] = f(x,y) \cdot F(t) \tag{10}$$

$f(x,y)$  is the spatial distribution function of the cubic shape load and  $F(t)$  is the time variation function. For the cylindrical shape load, an equivalent cubic shape load can be assumed as cubic shape load with rectangular  $2b \times 2b$  amplitude  $q$ , which is

$$f(x,y) = \begin{cases} q & \text{for } -b \leq x \leq b, -b \leq y \leq b \\ 0 & \text{another} \end{cases} \tag{11}$$

Then, the method of double Fourier transforms is utilized to determinate the spatial distribution coefficient  $\tilde{F}_{rm}$ .

$$f(x,y) = f(x) \cdot f(y) = \sum_r \sum_m \tilde{F}_{rm} \cos(k_r x) \cos(k_m y) \tag{12}$$

#### 5 Parameter identification of the bounded layer system

In the normal dynamic testing, a testing pulse is applied on the center of surface and the vertical displacements are measured from a series of sensors ( $S_1, S_2, \dots, S_n$ ) located at center and some distances away from the loading area. (Fig. 4)

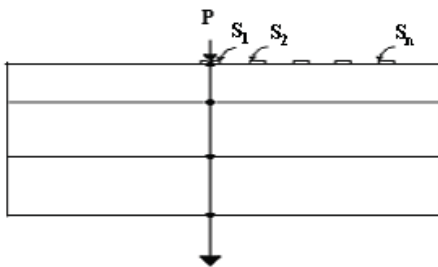


Figure 4: Measured locations of Geophone

Inverse calculation system should select one of optimization methods as an algorithm for parameter identification. Since the spectral element forward model is processed by a series of nonlinear

equations mentioned above, the parameter identification system should utilize nonlinear minimization techniques. Modified Powell hybrid algorithm is proposed to solve nonlinear equations in non-constrained optimization system.

#### 6 Modified Powell hybrid algorithm

The algorithm applies a hybrid between Quasi-Newton and Steepest Decent iteration techniques conforming to a step size criterion. The step size parameter  $\delta_k$ , the boundary of region of trust, is the factor to describe the type of iteration. In Powell method the search direction  $p_s$  is first calculated by the Quasi-Newton iteration:

$$\begin{aligned} J(x_k) q_k &= -p_s(x_k) \\ q_k &= -H(x_k) p_s(x_k) \\ \|q_k\| &\leq \delta_k \end{aligned} \tag{13}$$

Here  $p_s(x_k)$  is the objective function to be minimized,  $J(x_k)$  is the finite difference approximation of the Jacobian at the point  $x_k$ , and  $H(x_k)$  is its inverse. If the calculated point satisfies a certain criterion, the steepest descent will be used to calculate the next one. If the criterion is failed, the new search direction will be a hybrid between the Quasi-Newton and the steepest descent.

#### 7 Inverse calculation with nonlinear optimization

In the inverse calculation, inputting a proper fixed angle frequency ( $\omega_n$ ), the program starts with some initial guess of the unknown parameters such as layer E moduli. Parameter identification is performed by means of iterative comparison of the measured versus calculated results. The theoretical response results is derived from

$$[\tilde{u}_1 \ \tilde{u}_2 \ \dots \ \tilde{u}_i] = [\tilde{G}_{11} \ \tilde{G}_{21} \ \dots \ \tilde{G}_{i1}] \cdot \tilde{P}_1 \tag{14}$$

$[\tilde{u}_1 \ \tilde{u}_2 \ \dots \ \tilde{u}_i]$  is the nodal vertical displacement vector in frequency domain, and  $\tilde{P}_1$  is a unit vector. Then vertical displacements in frequency domain at nodes and the sensors' location are calculated as:

$$\tilde{u}_i^s(\omega_n) = \sum_{m=0}^{\infty} \sum_{r=0}^{\infty} \tilde{G}(z, k_r, k_m, \omega_n) \cdot \tilde{F}_{rm} \cdot \cos(k_r x(S_n)) \quad (15)$$

$x(S_j)$  is the distances from sensors to the center. Hence the objective function is expressed as the discrepancy between the measured and theoretical transfer function at the different location of sensors (Figure. 4). Minimizing procession gives Min:

$$p^s(\omega_n) = \left| \sum_{m=0}^{\infty} \sum_{r=0}^{\infty} \tilde{G}_{11} \cdot \tilde{F}_{rm} \cdot \cos(k_r x(S_j)) \right|_{theo} - |\tilde{u}_1^s(\omega_n)|_{meas} \quad (16)$$

The first absolute value given in the function represents the theoretical transfer function, while the second is the measured transfer function. If the difference is more than some selected minimum criterion, the iteration will continue until minimum criterion is satisfied. Then the parameter results are obtained by outputting. The algorithm of the program is as follows:

- 1 Program 3DSEP\_Back calculation
  - 2 Input  $\omega_n, x_0$
  - 3 Use FFT to transform  $F(t)$  and  $u^s(t)$  to  $\tilde{F}(\omega)$  and  $\tilde{u}^s(\omega)$
  - 4 Set  $x = x_0, \tilde{u}_1^s(\omega_n)_{theo} = 0$
  - 5 m\_Loop Do m=1, M
  - 6 r\_Loop Do r=1, R
  - 7 Form element stiffness matrices and global stiffness matrix
  - 8 Compute the theoretical transfer functions:
- $$\tilde{u}_1^s(\omega_n)_{theo} = \tilde{u}_1^s(\omega_n)_{theo} + \tilde{G}_{11} \cdot \tilde{F}_{rm} \cdot \cos(k_r x(S_j))$$
- 9 Enddo r\_Loop
  - 10 Enddo m\_Loop

- 11 Calculate the objective function:

$$p_s(x) = |\tilde{u}_1^s(\omega_n)|_{theo} - |\tilde{u}_1^s(\omega_n)|_{meas}$$

- 12 Start minimization
- 13 If  $(p_s(x) > \varepsilon)$
- 14 Determine new guess for x
- 15 Go to m\_Loop
- 16 Endif
- 17 Output
- 18 End program

## 8 Numerical Verification of inverse analysis

The typical FWD field measurement is used as the input data for inverse calculation. Figure 5 shows the typical FWD datum at measured point of a pavement structure. The structure consists of an asphalt layer (E = 2500 MPa and h = 150 mm), a subbase layer (E = 300 MPa and h = 350 mm) and subgrade layer (E = 100 MPa and h = ∞). Fig. 5(a) shows the measured load pulse, and Fig. 5(b) shows the measured vertical deflection of the pavement structure at the sensors from r = 0 to r = 1800. The minimization algorithm was used for identifying the materials' E modules of the three layers. The initial guess for the modules were: asphalt's E = 1000 MPa, subbase's E = 50 MPa and subgrade's E = 30 MPa, which represented about 30% of the actual values.

Table 1: Calculated parameters following various frequencies

Frequency (Hz)	Asphalt E(Mpa)	Subbase E(Mpa)	Subgrade E(Mpa)	Error (%)
14.01	2504	301	83	1.41
30.02	2500	306	80	0.67
68.04	2503	303	83	1.62
80.05	2500	312	89	5.08

The inverse calculation was processed at frequency ranging from 2 to 80Hz shown in Tab. 1. The convergence to minimum was less than 45 iterations. The longest iterative process only

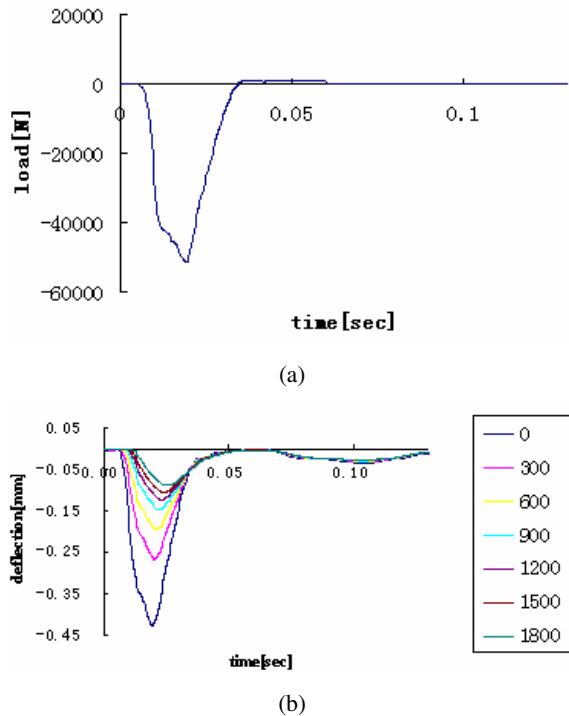


Figure 5: Typical FWD measurement data (a)load pulse (b) Measured surface vertical deflection

costs about 10 seconds. In order to avoid numerical ambiguities, it is recommended that the inverse calculation be performed by more than one frequency.

## 9 Backcalculation in CRCP testing pavement FWD measurement

Continuously Reinforced Concrete Pavement (CRCP) is a Portland cement concrete (PCC) pavement that has continuous longitudinal steel reinforcement and no intermediate transverse expansion or contraction joints. The pavement is allowed to crack in a random transverse cracking pattern and the cracks are held tightly together by the continuous steel reinforcement. In this project, the measured pavement have four layers, including Asphalt concrete, CRCP plate, semi-rigid subbase and soil subgrade. The CRCP pavement has two types of structures—Testing road 1 and Testing road 2. The cross-section of CRCP testing roads is shown in Fig.6, and the structure of them are drawn in Fig.7. In the structure of Testing road 1, the first two layers—SMA and

CDAC can be combined into one Asphalt layer due to the similar E modules. Corresponding to the structure of CRCP pavement, a flexible pavement is designed for the comparison. The geometrical and physical characteristics of the three kinds of structures are displayed in Tab. 2.

Backcalculations are performed in four layers of the structure, including AC layer, CRCP layer, semi-rigid subbase and soil subgrade. In Tab. 2, the thickness and Poisson's ratio of pavement are input as given parameters, and E module of every layer is calculated as outputting. As a comparison, the dynamic and static inverse methods are utilized for E module's backcalculation. Here, the dynamic inverse system applies 3D spectral element inverse dynamic algorithm, while the static inverse system is based on a typical static model subjected to a uniform load.

The backcalculation results of every layer's E modules are shown from Fig. 8 to Fig.11. The transverse axis of each figure is the number of measured points and the vertical axis expresses the inversed results of E modules. In the first layer (Fig. 8), the inversed E modules calculated by the dynamic method were more stable and close to the actual value than those by the static method. But the deference of the dynamic and static results was not very large. The static method still can give the relatively correct inversed-analytical results of AC layer. However, from Fig. 9 to Fig. 10, it was observed that the dynamic results were close to the measured E modules, whereas the static inverse resolution are much higher than accurate variables. It proved that the results of the static backcalculation were inaccurate in CRCP layer and semi-rigid subbase. The reason of this phenomena maybe is that the strength of those two layers are much larger than the first layer and the vagarious results of the static method often appear in relatively rigid layers. In the soil layer (Fig. 11), even the results of the dynamic method are not very stable. That means, for the limitation of FWD pulse's energy, the responsive signals received by FWD are not enough to achieve precise inversed results of the last layer in this project.

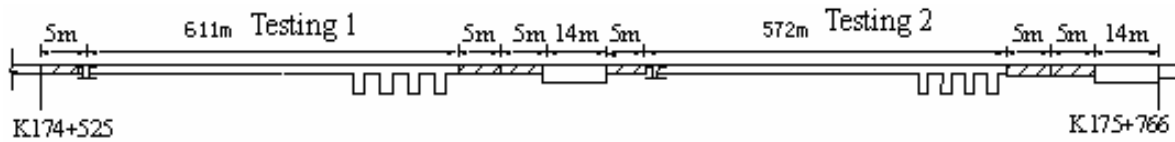


Figure 6: The cross-section of CPCP testing roads

Test road 1 (620m)	Test road 2 (580m)
4cm SMA-13	6cm SMA-13
6cm CDAC-20	
26cm CRCP	24cm CRCP
1 cm Asphalt glue	1 cm Asphalt glue
20cm Cement stabilized subbase	26cm Cement stabilized subbase
20cm Plaster and Soil subbase	20cm Plaster and Soil subbase

Figure 7: The structure of testing road 1 and testing road 2

Table 2: The geometrical and physical characteristics of the three structures

	Structure	Thickness (cm)	E (MPa)	Poisson's ratio
Test 1	AC layer	10	2000	0.35
	CRCP layer	26	30000	0.167
	Semi-rigid subbase	20	5000	0.20
	Soil subgrade	$\infty$	500	0.45
Test 2	AC layer	6	2000	0.35
	CRCP layer	24	30000	0.167
	Semi-rigid subbase	26	5000	0.20
	Soil subgrade	$\infty$	500	0.45
Flexible pavement	AC layer	25	2000	0.35
	Crushed rock layer	15	500	0.40
	Semi-rigid subbase	16	5000	0.20
	Soil subgrade	$\infty$	500	0.45

## 10 Conclusions

The three-dimensional layer spectral element is developed in this study for the analysis of multi-layered pavement system subjected to dynamic loading. Based on the spectral analysis, one element is adequate to describe one layer, so the number of the element meshes is equal to the number of the layers. The system is solved by the multi-summation over the frequencies and the

wavenumbers, which alleviates the inconvenience of the numerical calculation of infinite integration. The transformation from time to frequency domain is achieved by using FFT (Fast Fourier transforms), and procedures from frequency to time domain are done by means of IFFT (Inverse FFT). Hybrid Powell optimization is applied for the minimized determination of the discrepancy between theoretical and measured transfer function. The accuracy and efficiency were verified

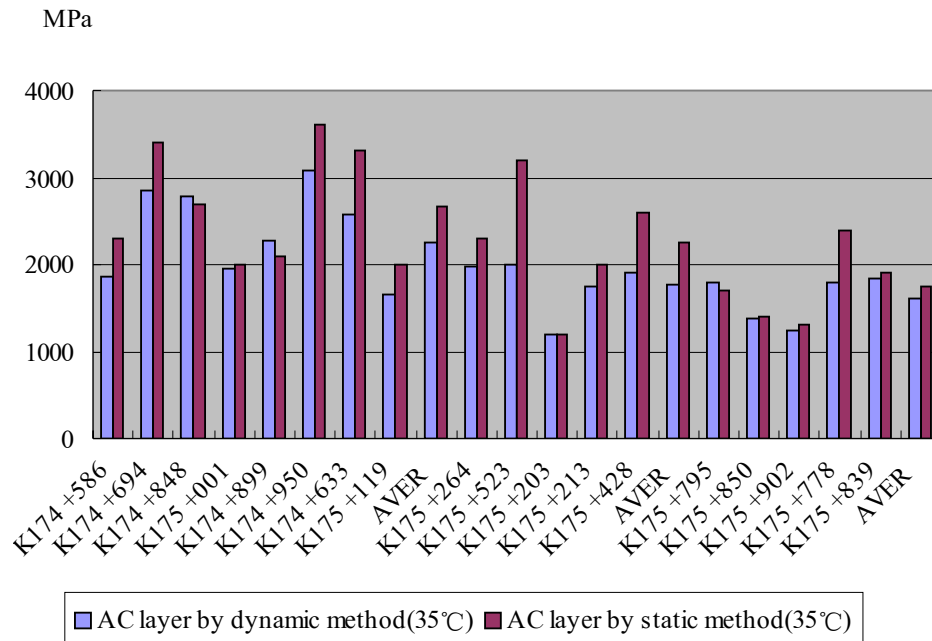


Figure 8: AC layer in 35° calculated by dynamic and static method

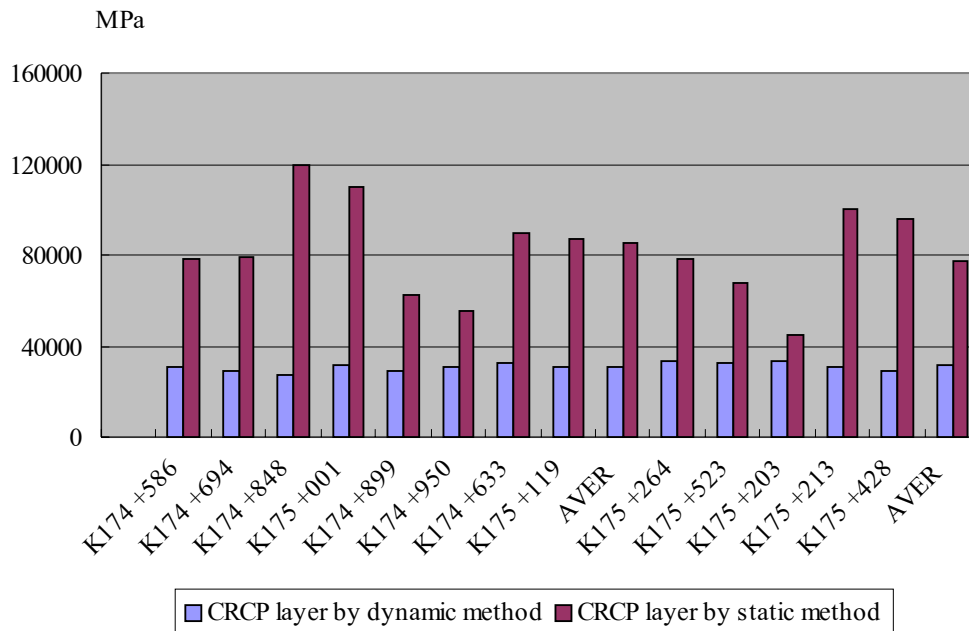


Figure 9: CRCP layer calculated by dynamic and static method

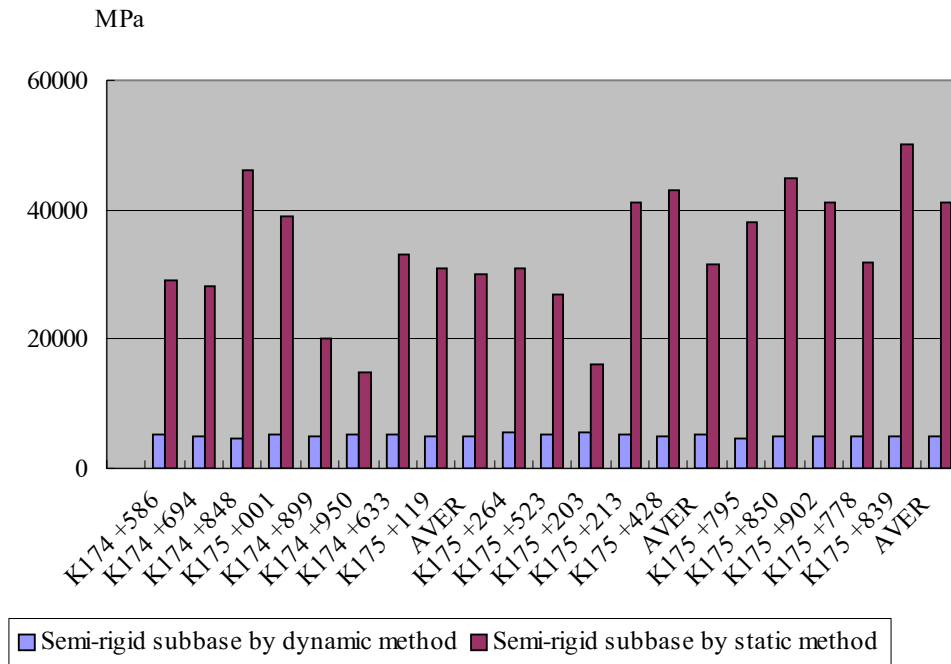


Figure 10: Semi-rigid subbase calculated by dynamic and static method

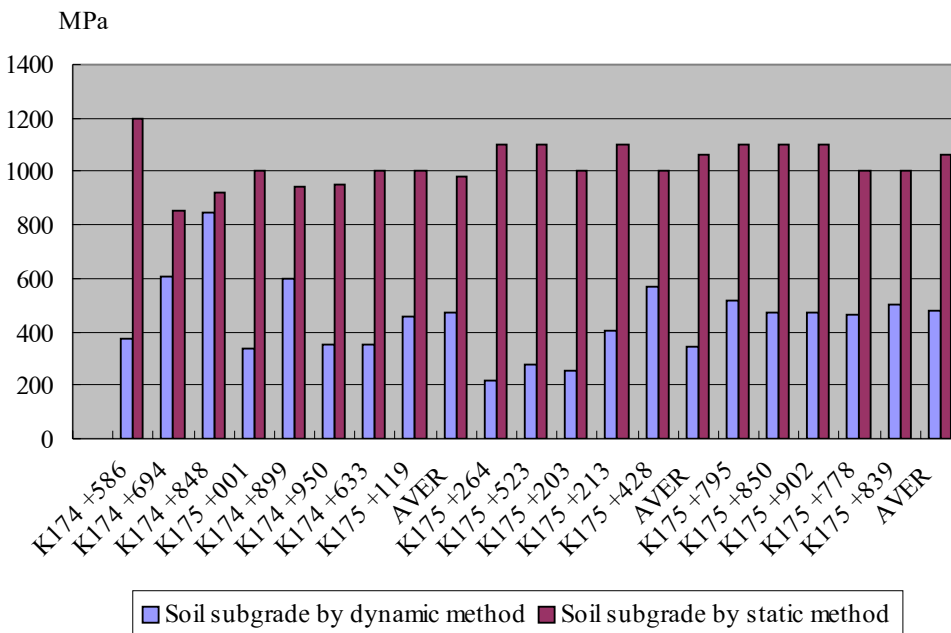


Figure 11: Soil subgrade calculated by dynamic and static method

by numerical examples both in the analytical forward and inverse calculations. In this article, the new dynamic method is utilized in CRCP pavement project. Through the backcalculation of the structural layers, it proved that the 3D spectral element method has great priority in evaluating relatively rigid pavement layers.

**Acknowledgement:** The authors would like to thank Prof. Hujian Ni and Dr. Qiao Dong for their cordial help.

## References

- Al-Khoury, R.; Scarpas, A.; Kasbergen, C.; Blaauwendraad, J.** (2001): Spectral element technique for efficient parameter identification of layered media, Part I: Forward calculation. *International Journal of Solids and Structures* vol. 38, pp. 1605–1623.
- Brigham, E.O.** (1988): The Fast Fourier Transform and Its Applications. *Prentice-Hall, Englewood Clis, NJ*.
- Dennis, J.E.; Schnabel, R.B.** (1983): Numerical Methods for Unconstrained Optimization and Nonlinear Equations, Prentice-Hall.
- Doyle, J.F.** (1997): Wave Propagation in Structures: Spectral Analysis using Fast Discrete Fourier Transforms. *Springer-Verlag, New York*.
- Gill, P.E.; Murray, W.; Wright, M.H.** (1981): Practical Optimization, Academic Press.
- Haskell, N.A.** (1953): The dispersion of surface waves on multilayered media. *Bull. Seism. Soc. Am.* vol.43, pp. 17-34.
- IMSL** (1997): Fortran Subroutine for Mathematical Applications, Math/Library, vol.1 and 2
- Kausel, E.; Roesset, J.M.** (1981): Stiffness matrices for layered soils. *Bull. Seism. Soc. Am.* vol. 71, pp.1743-1761.
- Kreyszig, E.** (1999): Advanced Engineering Mathematics, John Wiley Sons.
- Press, W.H.; Flannery, B.P.; Teukolsky, S.A.; Vetterling, W.T.** (1986): Numerical Recipes, The Art of Scientific Computing, Cambridge.
- Lamb, H.** (1904): On the propagation of tremors over the surface of an elastic solid, *philosophical transactions of royal society*, V. CCIII(1), pp.1-42.
- Rizzi, S.A.; Doyle, J.F.** (1992): Spectral analysis of wave motion in plane solids with boundaries, *Journal of Vibration and Acoustics*, vol. 114, pp.133-140.
- Rizzi, S.A.; Doyle, J.F.** (1992): A spectral element approach to wave motion in layered solids, *Journal of Vibration and Acoustics*, vol.114, pp.569-577.
- Scales, L.E.** (1985): Introduction to Non-Linear Optimization, Macmillan, Schoukens, J. and Pintelon, R., 1991. Identification of Linear Systems; a Practical Guideline to Accurate Modeling, Pergamon, Oxford.
- Thomson, W.T.**(1950): Transmission of elastic waves through a stratified solid media. *J. Applied Phys*, vol.21, pp.89-93.
- WMD-MISS**(1991): Backcalculation Software Package, User's manual, KOAC, WMD, Apeldoorn, Netherlands.
- Uzan, J.** (1994): Dynamic linear back calculation of pavement material parameters. *Journal of Transportation Engineering*, vol. 120, no. 1, pp. 109-126.
- Wu, Chun-Ying.; Liu, Xue-Yan.; Scarpas, A.; Ge, Xiu-Run.** (2006): Spectral Element Approach for Forward Models of 3D Layered Pavement. *CMES: Computer Modeling in Engineering and Sciences (CMES)*, vol.12, no.2, 149-157.